Pathology & Oncology Research | frontiers

TYPE Original Research
PUBLISHED 23 November 2026
DOI 10.3389/pore.2026.1612501

Check for updates

OPEN ACCESS

EDITED BY
József Tímár,
Semmelweis University, Hungary

*CORRESPONDENCE
István Szegedi,
iszegedi@med.unideb.hu

†These authors have contributed equally to this work

‡These authors have contributed equally to this work

RECEIVED 04 June 2026
REVISED 09 November 2026
ACCEPTED 12 November 2026
PUBLISHED 23 November 2026

CITATION
Kovács-Solymosi D, Mocsár G, Simon M, Gál K, Papp J, Macsi L, Kiss C, Kovács Á and Szegedi I (2026) Long-term dosimetric superiority of VMAT over 3D-CRT in pediatric focal brain irradiation: a comprehensive 15-year institutional analysis.
Pathol. Oncol. Res. 32:1612501.
doi: 10.3389/pore.2026.1612501

COPYRIGHT
© 2026 Kovács-Solymosi, Mocsár, Simon, Gál, Papp, Macsi, Kiss, Kovács and Szegedi. This is an open-access article distributed under the terms of the Creative Commons Attribution License (CC BY). The use, distribution or reproduction in other forums is permitted, provided the original author(s) and the copyright owner(s) are credited and that the original publication in this journal is cited, in accordance with accepted academic practice. No use, distribution or reproduction is permitted which does not comply with these terms.

Long-term dosimetric superiority of VMAT over 3D-CRT in pediatric focal brain irradiation: a comprehensive 15-year institutional analysis

Dóra Kovács-Solymosi[1†], Gábor Mocsár[1†], Mihály Simon[1], Kristóf Gál[1], Judit Papp[1], Lilla Macsi[2], Csongor Kiss[2], Árpád Kovács[1‡] and István Szegedi[2*‡]

[1]Department of Oncoradiology, Faculty of Medicine, University of Debrecen, Debrecen, Hungary, [2]Department of Pediatrics, Division of Pediatric Hematology and Oncology, Faculty of Medicine, University of Debrecen, Debrecen, Hungary

Background/objectives: Minimizing radiation-induced late effects is critical in pediatric neuro-oncology, where long life expectancy is associated with treatment-related toxicity. We evaluated the 15-year institutional transition from three-dimensional conformal radiotherapy (3D-CRT) to volumetric modulated arc therapy (VMAT) and compared their dosimetric performance in pediatric focal brain radiotherapy (FBRT).

Methods: Between 2011 and 2025, 27,393 patients were treated, including 175 pediatric cases (≤18 years). FBRT cases were selected for dosimetric analysis because they are the most common pediatric brain irradiation at our institution and involve small-to-medium targets located near radiosensitive critical structures, enabling a sensitive comparison of technique-dependent dosimetric differences. FBRT plans from 27 patients were analyzed (3D-CRT: n = 13; VMAT: n = 14) using a unified script-based workflow in RayStation combined with a standardized AI-based auto-segmentation tool. Metrics included V95%, homogeneity index (HI), conformity index (CI), and high-dose spillage (V102%). Exploratory organ at risk (OAR) analysis was performed in a more restricted prescription uniform subgroup. In addition, overall survival (OS) was evaluated using available clinical follow-up data from FBRT patients.

Results: VMAT significantly reduced high-dose volumes (V102%: 0.01% vs. 0.78%, $p = 3.8 \times 10^{-4}$), improved conformity (CI: 0.85 vs. 0.64, p = 0.008) and homogeneity (HI: 1.07 vs. 1.10, p = 0.048) compared with 3D-CRT. Target coverage was comparable. OAR analysis showed consistently reduced maximum doses to the optic chiasm and pituitary gland. No statistically significant difference in overall survival was observed between treatment techniques (p = 0.26).

Conclusion: Overall, our study demonstrates that the application of VMAT in pediatric focal brain irradiation improves the precision of dose distribution and may contribute to reducing long-term neurocognitive and endocrine toxicities. These findings support the clinical use of VMAT, with the potential to reduce late treatment-related toxicity in the pediatric patient population.

KEYWORDS
3D-CRT, dosimetric comparison, focal brain irradiation, pediatric brain radiotherapy, VMAT

Introduction

Radiotherapy is essential in treating pediatric tumors. Optimal treatment requires delivering a sufficient dose to the target while minimizing exposure to surrounding healthy structures, as even small reductions in unnecessary irradiation can lessen late effects such as neurocognitive decline [1, 2], endocrine dysfunction [3, 4], sensory deficits [5, 6], impaired craniofacial growth, facial asymmetry, dental and skeletal abnormalities [7, 8]. Continued refinement of radiotherapy techniques is therefore critical for improving long-term outcomes in children [9, 10]. Advances in treatment planning have enhanced dose conformality and normal-tissue sparing. Three-dimensional conformal radiotherapy (3D-CRT), the standard approach for a long time, provides reliable target coverage but is limited in shaping dose around complex intracranial anatomy [11–13]. Volumetric modulated arc therapy (VMAT) offers superior conformality and homogeneity through continuous modulation of beam parameters, though increased modulation may redistribute low- and intermediate-dose exposure [14–18]. Pediatric brain tumors often lie near highly radiosensitive structures such as the optic pathway, brainstem, cochleae, and endocrine organs, making advanced planning techniques that reduce high-dose exposure particularly valuable. This study provides a comprehensive single-institution review of pediatric radiotherapy practice over more than a decade. We assessed temporal trends in the use of 3D-CRT and VMAT and performed a detailed dosimetric comparison of clinically delivered pediatric focal brain radiotherapy plans. In addition, an overall survival analysis was conducted using available follow-up data. By examining target coverage, homogeneity, conformity, high-dose spillage, and organ-at-risk doses, this work offers insight into technique-specific advantages and supports optimization of radiotherapy for pediatric patients.

Materials and methods

Pediatric study design

To identify the pediatric subgroup (aged ≤18 years), clinical records of all patients treated at our institution between 2011 and 2025 were reviewed. Patient demographic data, including age at treatment and year of treatment, were extracted from the institutional database (MOSAIQ, Elekta AB, Stockholm, Sweden). The pediatric cohort was further categorized according to the anatomical region of irradiation. The following categories were defined: Brain, Craniospinal Irradiation (CSI), Head and Neck, Thorax, Abdomen, Pelvis, and Other. The Other category included anatomical regions not encompassed by the predefined groups (e.g., upper and lower limbs). To evaluate how the use of three-dimensional conformal radiotherapy (3D-CRT) and volumetric modulated arc therapy (VMAT) in pediatric patients has evolved at the institutional level between 2011 and 2025, the pediatric cohort was categorized according to the treatment technique used (3D-CRT or VMAT), with classification verified through manual review of the corresponding treatment plans. For pediatric patients receiving brain radiotherapy, treatments were further classified as whole-brain radiotherapy (WBRT) when the entire brain was included in the treatment volume, or focal brain radiotherapy (FBRT) when irradiation targeted a localized intracranial region.

Dosimetric analysis

Pediatric treatment plans originally generated in Oncentra (Elekta AB, Stockholm, Sweden) or Pinnacle^3 (version 9.2; Philips Medical Systems, Fitchburg, WI, USA) were calculated using the collapsed cone convolution (CCC) algorithm and subsequently imported into RayStation 11B (RaySearch Laboratories AB, Stockholm, Sweden) for advanced dosimetric analysis using script-based workflows. For the analyses, FBRT was selected as the primary analytical subgroup because it represents the most frequent pediatric brain irradiation indication at our institution and provides small-to-medium target volumes where conformity-driven dosimetric differences between techniques are most pronounced. All associated pediatric CT datasets were recontoured using a commercially available deep learning–based auto-segmentation platform (MVision AI, Helsinki, Finland) to ensure consistent and standardized structure delineation and naming across all cases. The following organs and structures were segmented: brain, brainstem, body contour, bilateral carotid arteries, cochleae, eyes (including anterior and posterior segments), lacrimal glands, lenses, optic nerves, optic chiasm, parotid glands, pituitary gland and pituitary fossa, face, spinal canal, and spinal cord. Original clinical and planning target volume contours were preserved without modification and used uniformly throughout the analysis.

Custom Python scripts were developed within the RayStation environment to automate contour creation using ROI algebra, as well as dosimetric data evaluation and extraction. Standard dose–volume metrics were collected at the prescription dose level to compare target coverage, dose homogeneity, conformity, low- and high-dose spillage between the two radiotherapy techniques. Target coverage was quantified as the percentage of the planning target volume (PTV) receiving at least 95% of the prescribed dose (V95%). Low dose exposure was assessed using V5%, defined as the percentage of the external volume excluding the target that received at least 5% of the prescribed dose. High-dose spillage was defined as the volume of external minus target volume receiving ≥102% of the prescribed dose (V102%). Dose uniformity within the target was assessed using the Homogeneity Index (HI), defined as $HI = D5/D95$ [19, 20], where $D5$ and $D95$ represent the doses received by 5% and 95% of the target volume, respectively. Values closer to 1 indicate better dose homogeneity. The Conformity Index (CI) [21, 22] was used to quantify the agreement between the prescribed isodose volume and the target volume, with values approaching 1 indicating optimal conformity. Maximum and mean doses were also extracted for all delineated structures. The unified script-driven workflow in RayStation, combined with standardized auto-segmentation, was applied to all cases to minimize inter-observer variability and enhance methodological consistency and reproducibility.

Overall survival analysis

Overall survival (OS) was calculated for the 3D-CRT and VMAT groups. OS was defined as the interval between the start of

TABLE 1 Distribution of pediatric radiotherapy cases by anatomical body site.

Body site	n (%)
Brain	60 (34.3%)
CSI	33 (18.9%)
Head and neck	32 (18.3%)
Thorax	22 (12.6%)
Abdomen	16 (9.1%)
Other	15 (8.6%)
Pelvis	9 (5.1%)

Patients with irradiation to multiple body sites were included in each corresponding body-site category; therefore, the total number of observations and percentages exceed 100%.

radiotherapy and the date of death or, in the absence of a documented death event, the date of last follow-up (censored observation). Patients with missing follow-up information were excluded from the survival analysis. Survival rates at predefined time points (12, 24, and 60 months) were estimated, and differences between treatment groups were evaluated using a two-sided log-rank test.

Statistical analysis

For descriptive statistics characterizing the age distribution of the overall population and the pediatric cohort, the following parameters were calculated: mean ± standard deviation (SD), median, first and third quartiles (Q1–Q3), interquartile range (IQR), minimum and maximum values, and the 95% confidence interval (CI; lower and upper bounds). Statistical comparisons of dosimetric parameters between 3D-CRT and VMAT plans were performed using two-sided Mann–Whitney U tests. For each group, the 95% confidence intervals of medians were estimated using nonparametric bootstrap resampling (5000 iterations). All statistical analyses were conducted in MATLAB (R2024b; The MathWorks, Inc., Natick, MA, USA).

Ethical statement

This study was conducted in accordance with the Declaration of Helsinki. The study protocol was reviewed and approved by the Medical Research Council Scientific and Research Ethics Committee (ETT-TUKEB, Hungary; approval number: BM/6038-1/2024, date of approval: 7 March 2024). Due to the retrospective nature of the study and the use of fully anonymized dosimetric data, the requirement for informed consent was waived by the Ethics Committees.

Results

Patient characteristics and body-site distribution

A total of 15 years of patient data were analyzed to characterize age-distribution patterns and annual case volumes for both the overall and pediatric populations. Of the 27,393 patients treated during the study period, 175 (0.64%) were pediatric patients (≤18 years). The pediatric cohort had a mean age of 9.55 ± 5.62 years (95% CI: 8.71–10.39), a median age of 9 years (IQR: 4–15 years), and an age range of 1–18 years. Because this study focused on the dosimetric analysis of focal brain radiotherapy (FBRT), the pediatric cohort (n = 175) was subsequently refined using anatomical body-site classification to identify cases relevant to the analysis. The distribution of pediatric radiotherapy cases by anatomical body site is summarized in Table 1. Brain irradiation represented the most frequent category (n = 60, 34.3%), followed by craniospinal irradiation (n = 33, 18.9%) and head and neck irradiation (n = 32, 18.3%). Because individual patients could receive treatment involving multiple anatomical regions, body-site categories were not mutually exclusive.

Radiotherapy technique utilization

To evaluate temporal changes in the institutional use of three-dimensional conformal radiotherapy (3D-CRT) and volumetric modulated arc therapy (VMAT) from 2011 to 2025, the pediatric cohort was categorized according to treatment technique. Temporal trends in radiotherapy use within the pediatric population are shown in Figure 1. The annual numbers of pediatric patients treated with 3D-CRT and VMAT are presented in Figures 1A,B, respectively.

During the early years of the study period, pediatric radiotherapy treatments were predominantly delivered using three-dimensional conformal radiotherapy (3D-CRT). Over time, however, the use of VMAT increased substantially, especially in the later years. The proportional distribution of treatment techniques across the 2011–2025 period is shown in Figure 1C and clearly demonstrates this transition. Together, these trends reflect the gradual institutional adoption of more advanced treatment planning techniques in pediatric radiotherapy.

Pediatric brain tumors represented the largest subgroup in our institution between 2011 and 2025 (n = 60). Excluding whole-brain radiotherapy (WBRT) cases, the FBRT cohort exhibited substantial anatomical and clinical heterogeneity, spanning diverse tumor locations, target volumes, and proximities to critical structures. We hypothesized that potential dosimetric differences between treatment techniques would be most apparent in small-to medium-sized target volumes, as typically encountered in FBRT. Therefore, within the brain irradiation cohort, we selected patients treated with focal brain radiotherapy (FBRT) for more detailed analysis. The distribution of pediatric patients receiving either FBRT or WBRT is summarized in Table 2. Among the 60 pediatric brain radiotherapy cases identified, FBRT constituted the majority (n = 39), whereas WBRT was administered in 21 cases. Within the FBRT subgroup, 3D-CRT was used in 22 patients and VMAT in 17 patients.

Due to the possible proximity of critical structures—such as the optic chiasm and optic nerves—to the clinical target volumes, the FBRT cohort provides a meaningful basis for comparing technique-dependent differences in conformity, homogeneity, and high-dose spillage. These dosimetric parameters are especially important in pediatric neuro-oncology, where even small improvements may help reduce the risk of long-term neurocognitive, endocrine, and sensory toxicities. For these reasons, FBRT was selected as the primary subgroup for evaluating the dosimetric performance of 3D-CRT versus VMAT.

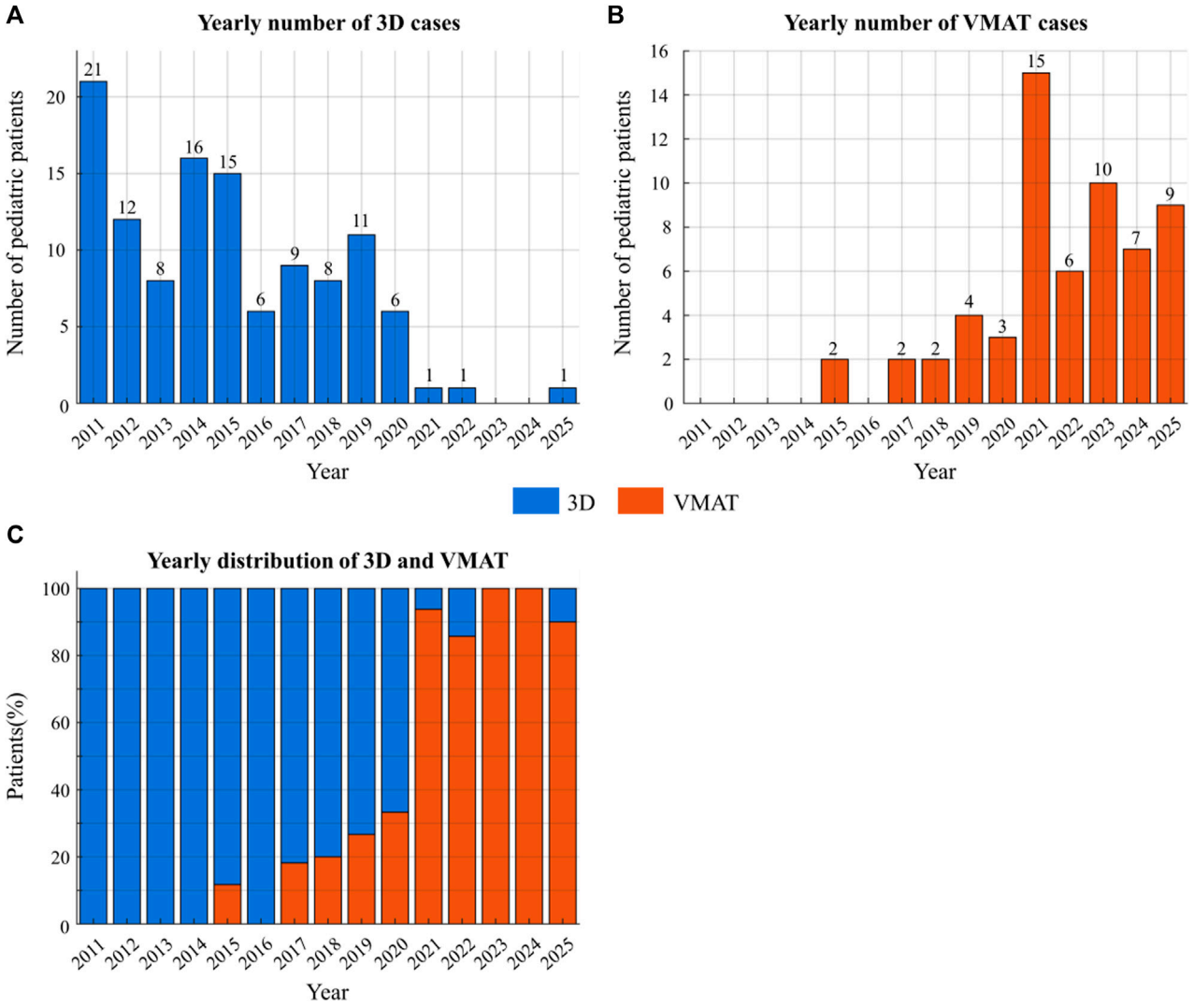


FIGURE 1
Technique utilization over time in pediatric radiotherapy: **(A)** Annual number of pediatric patients treated with three-dimensional conformal radiotherapy (3D-CRT). Bars indicate absolute case counts per year. **(B)** Annual number of pediatric patients treated with volumetric modulated arc therapy (VMAT). **(C)** Yearly distribution of radiotherapy techniques displayed as a 100% stacked bar chart. Bars represent the relative proportion of treatments delivered with 3D-CRT and VMAT in each calendar year.

TABLE 2 **Distribution of pediatric patients receiving brain radiotherapy according to treatment volume and radiotherapy technique.**

Treatment type	N	FBRT technique	N
FBRT (focal brain radiotherapy)	39	3D-conformal radiotherapy (3D-CRT)	22
WBRT (whole brain radiotherapy)	21	Volumetric modulated arc therapy (VMAT)	17
Total	60	Total (FBRT only)	39

Representative dose distribution comparison

To support the dosimetric evaluation of focal brain radiotherapy (FBRT) and the comparison between 3D-CRT and VMAT techniques, a representative pediatric patient with both plan types available was selected to visually illustrate differences in dose distribution. The prescribed dose was 54 Gy delivered in 30 fractions. For the clinical 3D-CRT plan, six coplanar 6 MV photon beams were used, each delivered with a single segment. Gantry angles were evenly distributed at 230°, 270°, 300°, 50°, 90°, and 120°, with monitor units (MU) per beam ranging from 21.8 to 34.6 MU.

For the demonstrative VMAT plan, a single 6 MV volumetric modulated arc therapy arc was employed. The arc spanned a full rotation—from 181° to 180° in a clockwise direction—providing complete 360° coverage. A total of 317.10 MU was delivered, and the plan consisted of 91 segments, enabling continuous modulation of dose rate, gantry speed, and multileaf collimator (MLC) positions throughout the arc.

A representative example of focal brain radiotherapy (FBRT) dose distributions for the 3D-CRT and VMAT plans is shown in Figure 2. Transversal (Figure 2A), sagittal (Figure 2B), and coronal (Figure 2C) views are presented for both techniques, accompanied by a voxel-wise dose-difference map (ΔDose). Across all three anatomical planes, the VMAT plan demonstrated visibly improved dose conformity to the target volume compared with 3D-CRT. In contrast, the 3D-CRT plan exhibited a broader lateral spread of intermediate and high isodose levels, most prominently in the coronal and transverse views. The ΔDose maps further confirmed that higher peripheral dose deposition was predominantly associated with the 3D-CRT technique, whereas VMAT consistently reduced dose exposure to the surrounding normal tissues. In the sagittal plane, VMAT additionally produced a sharper anterior–posterior dose fall-off relative to the target. Overall, this representative pediatric case illustrates that VMAT provides more conformal target coverage and superior sparing of adjacent tissues compared with conventional 3D-CRT.

Dosimetric comparison of 3D-CRT and VMAT for focal brain radiotherapy

To quantify the visually observed differences in dose distribution between 3D-CRT and VMAT plans in selected FBRT cases, a custom-written Python script was used to extract dose–volume data and compute all relevant dosimetric indices in a

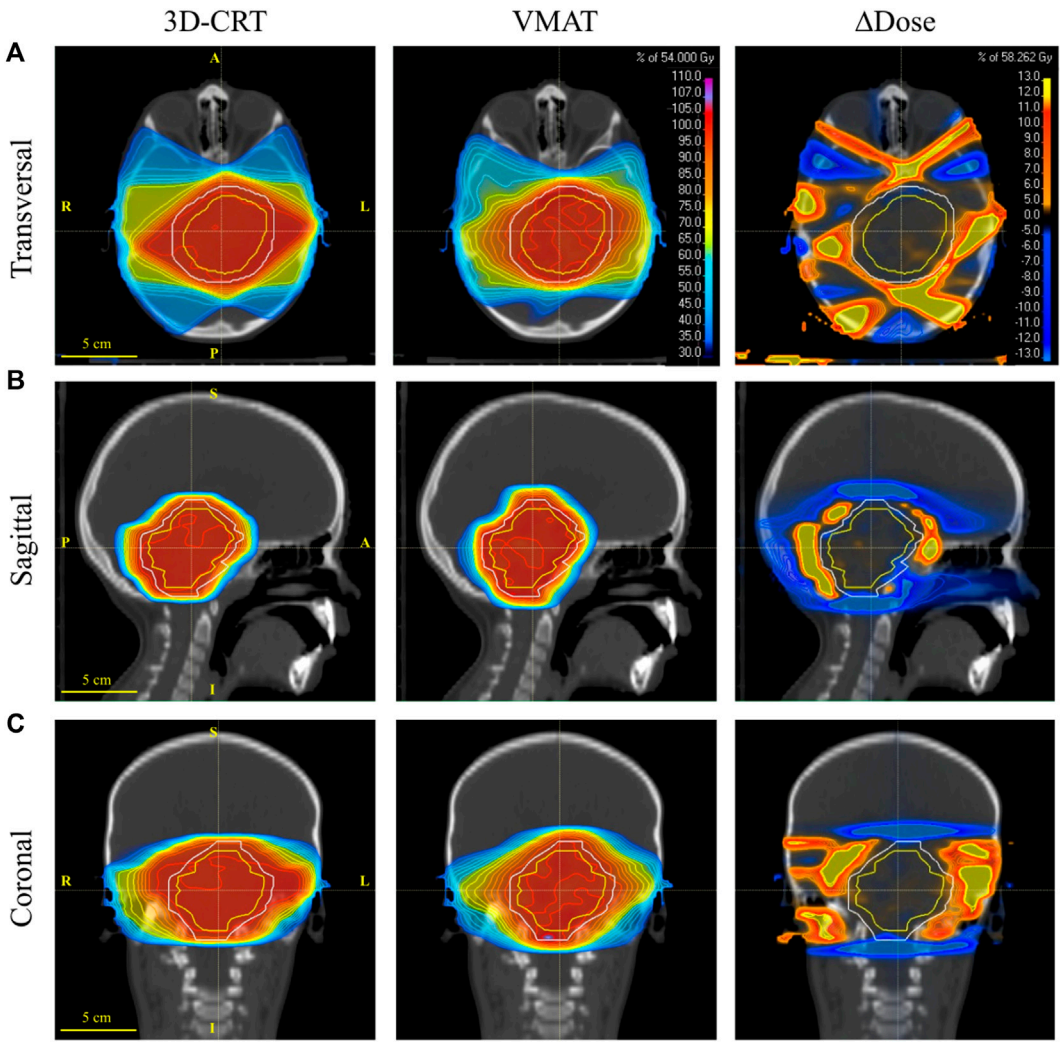


FIGURE 2
Representative comparison of 3D-CRT and VMAT dose distributions in a selected pediatric FBRT case: Dose distributions are shown in three orthogonal planes: **(A)** transverse, **(B)** sagittal, and **(C)** coronal views. The left column illustrates the dose distribution of the 3D-CRT plan, the middle column shows the VMAT plan, and the right column presents the voxel-wise dose-difference (ΔDose) map between the two techniques. Isodose lines are overlaid on the planning CT images for spatial reference. The high-dose target region is depicted in red, with surrounding colors indicating progressively lower dose levels. In the ΔDose maps, warm colors denote regions receiving higher dose in the 3D-CRT plan, whereas cool colors indicate regions receiving higher dose in the VMAT plan.

10.3389/pore.2026.1612501

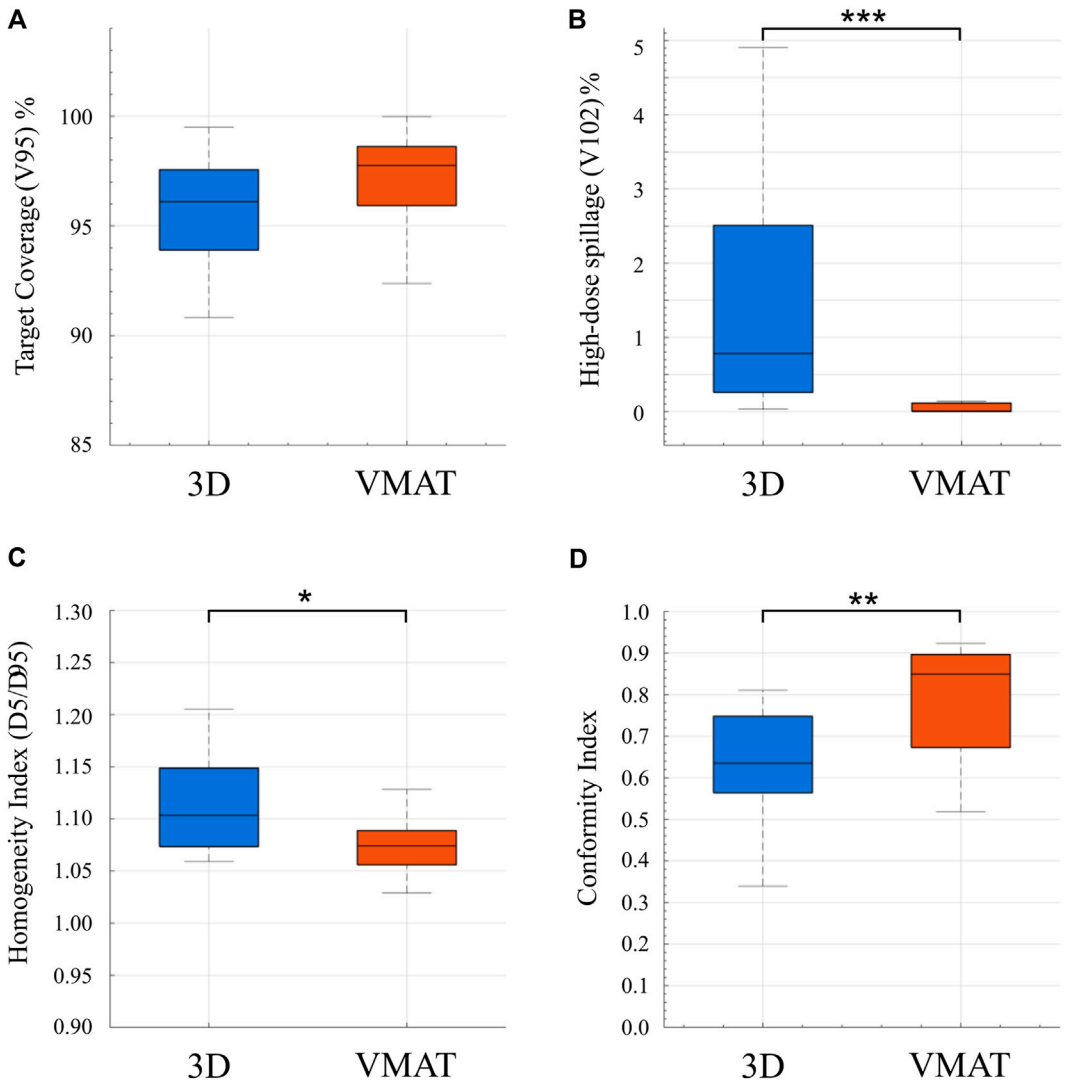


FIGURE 3
Dosimetric comparison between 3D-conformal radiotherapy and VMAT: Boxplots illustrate differences in target coverage, high-dose spillage, dose homogeneity, and conformity index between 3D-CRT and VMAT plans. The upper panels show **(A)** target coverage at 95% of the prescribed dose (V95%) and **(B)** the volume of external tissue receiving ≥102% of the prescribed dose (V102%). The lower panels present **(C)** the Homogeneity Index (HI = D5/D95) and **(D)** the Conformity Index (CI), both evaluated at the prescription dose level. Boxes represent the interquartile range (IQR), whiskers indicate the full range excluding outliers, and the median is shown as a horizontal line. Blue boxes denote 3D-CRT, and orange boxes denote VMAT. *: $p < 0.05$; **: $p < 0.01$; ***: $p < 0.001$.

standardized manner. The analysis included V95%, V102%, V5%, conformity index (CI), and homogeneity index (HI), evaluated in pediatric patients treated with 3D-CRT (n = 13) and VMAT (n = 14). These plans represent all dosimetrically available, independent, and clinically delivered treatment plans suitable for analysis out of the total cohort of 39 FBRT cases. Across all metrics, VMAT demonstrated clear dosimetric advantages, including improved target coverage, reduced high-dose spillage, and superior dose homogeneity and conformity compared with 3D-CRT. The distributions of these dosimetric parameters are shown in Figure 3. Median target coverage (V95%, Figure 3A) was 96.10 (95% CI: 93.90-97.56) for 3D-CRT and 97.75 (95% CI: 95.93-98.62) for VMAT, corresponding to a relative increase of 1.7% with VMAT. However, this difference was not statistically significant ($p = 0.19$), indicating that both techniques achieved adequate prescription-dose coverage.

VMAT resulted in significantly lower high-dose exposure, as reflected by a reduced V102% compared with 3D-CRT ($p = 3.8 \times 10^{-4}$) (Figure 3B). Median values decreased from 0.78 (95% CI: 0.28-2.34) for 3D-CRT to 0.01 (95% CI: 0.00-0.09) for VMAT, corresponding to a relative reduction of 99.1%. These findings are consistent with the overall pattern that VMAT more effectively limits high-dose spillage to adjacent healthy tissues. Low-dose exposure, expressed as V5% of the external volume, showed no statistically significant difference between techniques ($p = 0.6$). The median V5% was 54.60 (95% CI: 40.92-68.93) for 3D-CRT and 45.84 (95% CI: 35.51-66.81) for VMAT, corresponding to an approximately 16.0% relative reduction with VMAT (data not shown).

10.3389/pore.2026.1612501

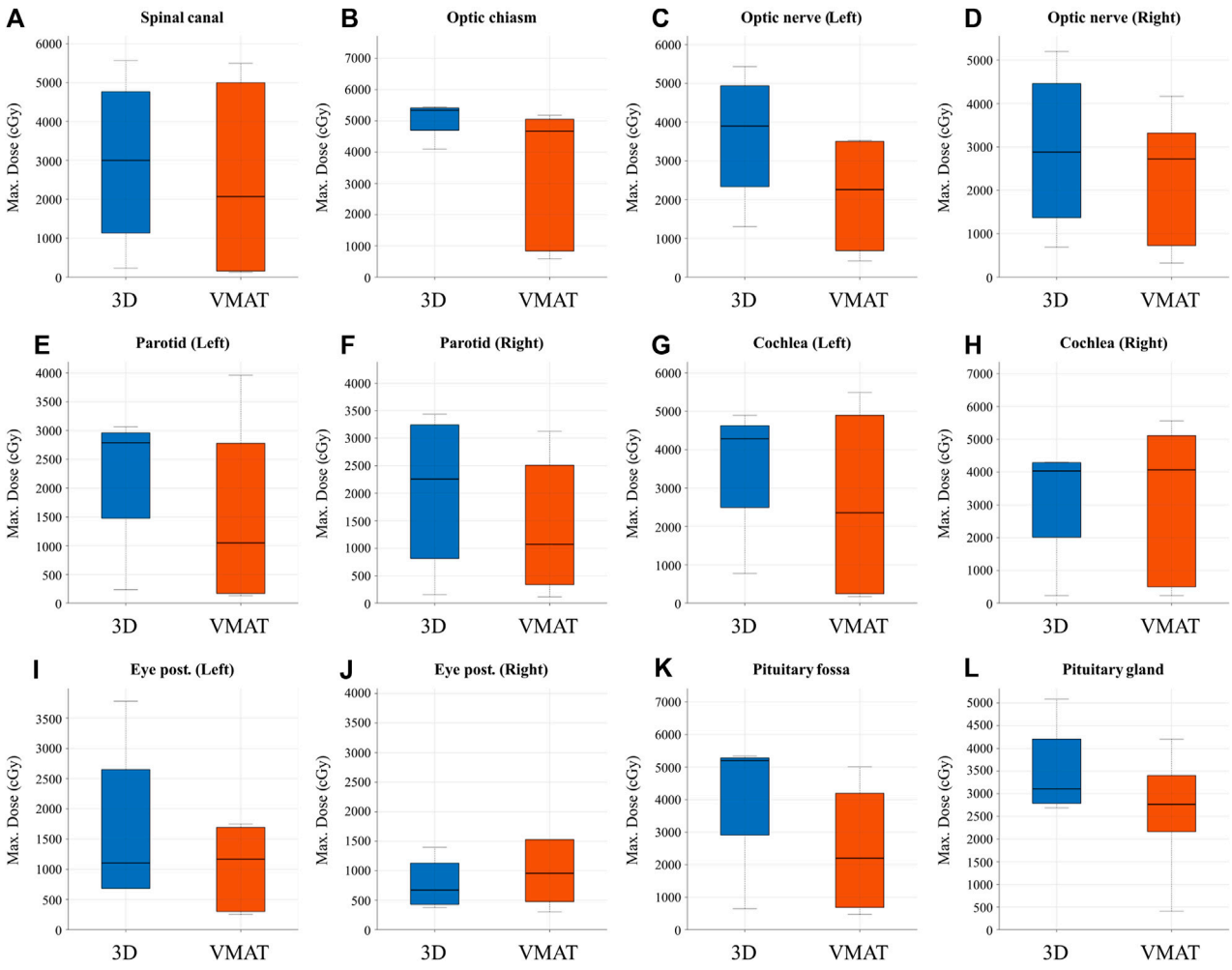


FIGURE 4
Distribution of maximum doses (cGy) delivered to selected organs at risk (OARs) for pediatric patients treated with 3D-CRT and VMAT. Box plots display the median, interquartile range, and full data range for each structure. OARs shown include **(A)** the spinal canal, **(B)** optic chiasm, **(C,D)** left and right optic nerves, **(E,F)** left and right parotid glands, **(G,H)** left and right cochleae, **(I,J)** left and right posterior eye segments, and **(K,L)** the pituitary fossa and gland. Comparisons were restricted to patients receiving a uniform prescription dose of 54 Gy.

Dose homogeneity describes how uniformly the radiation dose is distributed within the target volume. A homogeneity index value close to 1 indicates a nearly uniform dose distribution, whereas higher values reflect the presence of hot and cold spots. VMAT significantly improved dose homogeneity (Figure 3C), as demonstrated by lower homogeneity index values (HI = D5/D95) compared with 3D-CRT ($p = 0.048$). Median HI values decreased from 1.10 (95% CI: 1.07–1.13) for 3D-CRT to 1.07 (95% CI: 1.06–1.09) for VMAT, corresponding to a relative reduction of 2.7%. These results indicate that VMAT achieved a more homogeneous dose distribution within the target volume.

Finally, conformity describes how well the high-dose region matches the shape and extent of the target volume. VMAT again showed superior performance, with significantly higher conformity index (CI) values compared with 3D-CRT ($p = 0.008$) (Figure 3D). Median CI values increased from 0.64 (95% CI: 0.57-0.74) for 3D-CRT to 0.85 (95% CI: 0.67-0.90) for VMAT, corresponding to a relative improvement of 33.7%. These findings indicate that VMAT achieved a dose distribution that more closely conformed to the target volume. Overall, while target coverage was comparable between techniques, VMAT provided superior dose homogeneity and conformity, along with reduced high-dose volumes.

Organ at risk dose comparison

As VMAT demonstrated better performance compared to 3D-CRT in a pediatric FBRT cohort, we aimed to further investigate, beyond standard dosimetric parameters, whether differences could also be observed in terms of organ-at-risk (OAR) sparing. Due to heterogeneity in prescribed doses across pediatric patients, direct comparisons based on maximum dose would have been difficult to interpret; therefore, comparisons of maximum and mean doses to organs at risk (OARs) were restricted to cases with a uniform prescription of 54 Gy in 27 or 30 fractions. In this analysis, ten pediatric patients could be included (n = 4 for 3D-CRT and n = 6 for VMAT), consequently the relatively small cohort sizes reflect the rarity of pediatric brain tumors combined with the strict inclusion criteria applied. Accordingly, this OAR analysis should be

TABLE 3 Survival analysis according to radiotherapy technique.

Parameter/Treatment type	3D-CRT	VMAT
Patients	8	15
Deaths, n (%)	2 (25.0%)	6 (40.0%)
Censored, n (%)	6 (75.0%)	9 (60.0%)
12-month OS, %	87.5	92.9
24-month OS, %	87.5	61.9
60-month OS, %	75.0	46.4
Log-rank chi-square	1.25	
Log-rank p	0.26	

considered exploratory and hypothesis-generating. Maximum and mean doses were extracted for all relevant OARs, including the carotid arteries, brain, brainstem, cochleae, anterior and posterior eye segments, whole eyes, face, pituitary gland and pituitary fossa, lacrimal glands, lenses, optic chiasm, left and right optic nerves, parotid glands, spinal canal, and spinal cord. Figure 4 displays the distribution of maximum doses (cGy) delivered to selected OARs across the two techniques.

Across the evaluated organs at risk, VMAT consistently demonstrated a lower maximum dose compared with 3D-CRT. This pattern was most evident in the optic pathway structures, where several clinically relevant reductions were observed. For the optic chiasm, the median maximum dose decreased by 12.5% ($p = 0.11$). Similar dose-lowering trends were noted for the left and right optic nerves, the median values decreased by 42% ($p = 0.26$) and 5.5% ($p = 0.76$) respectively, with VMAT plans showing narrower dose distributions and lower upper-range values. Beyond the optic pathway, VMAT also tended to reduce maximum doses to several additional OARs, including the cochleae (Left: 44.9%, $p = 0.61$), parotid glands (62.4%, $p = 0.48$ and 52.5%, $p = 0.61$), and posterior eye segments. Although the magnitude of reduction varied by structure, VMAT generally produced more favorable dose profiles, with fewer high-dose volumes. In contrast, 3D-CRT plans exhibited broader variability and higher maximum dose values across multiple OARs.

Overall, VMAT showed a general tendency toward reduced maximum doses across several clinically important structures, particularly within the optic system, parotid glands, and pituitary region. A key limitation of this analysis is the heterogeneity of the clinical FBRT cases included, which could not be averaged out due to the strict inclusion criteria and resulting small sample size. Consequently, variations in tumor size, location, and anatomical complexity may have influenced dose distributions independently of the treatment technique. Given these constraints, and the limited number of evaluable patients, the findings should be interpreted with caution and regarded as exploratory.

Survival analysis

In addition to characterizing the dosimetric differences between 3D-CRT and VMAT, we aimed to investigate whether the observed improvements in FBRT plan quality could translate into a measurable survival benefit. Therefore, a survival analysis was performed using all available clinical follow-up data from FBRT cases to evaluate potential differences in overall survival between the two treatment techniques.

The analysis included 23 patients, of whom 8 were treated with 3D-CRT and 15 with VMAT (Table 3). During follow-up, 2 deaths occurred in the 3D-CRT group and 6 in the VMAT group, while 6 and 9 patients, respectively, were censored. The estimated 12-month overall survival (OS) rates were 87.5% for 3D-CRT and 92.9% for VMAT. At 24 months, the corresponding OS rates were 87.5% and 61.9%, while the 60-month OS rates were 75.0% and 46.4%, respectively. The median OS was not reached in the 3D-CRT cohort due to the limited number of events, whereas it was estimated at 44.6 months in the VMAT cohort. Kaplan–Meier analysis demonstrated no statistically significant difference in overall survival between the two treatment techniques (log-rank $\chi^2 = 1.25$, $p = 0.26$).

Discussion

This single-institution analysis provides a comprehensive evaluation of radiotherapy practice patterns and dosimetric outcomes in pediatric brain irradiation over a 15-year period. Given the frequent proximity of critical organs—such as the optic chiasm and optic nerves—to the target volumes, the FBRT cohort represents a particularly suitable model for detailed dosimetric evaluation. To ensure methodological robustness, all plans were analyzed using a unified script-based workflow in RayStation with standardized AI-based auto-segmentation, thereby minimizing inter-observer variability and enhancing reproducibility as previously demonstrated in brain radiotherapy workflows [23–26]. Our data demonstrate a transition from 3D-CRT to VMAT in routine clinical practice and show that VMAT offers measurable dosimetric advantages in pediatric focal brain radiotherapy (FBRT).

Our data demonstrate that VMAT achieves markedly superior target conformity compared with 3D-CRT (CI: 0.85 vs. 0.64, $p = 0.008$), accompanied by improved dose homogeneity and a substantial reduction in high-dose spillage (V102%: 0.01% vs. 0.78%, $p = 3.8 \times 10^{-4}$). Importantly, target coverage (V95%) remained comparable between techniques, indicating that VMAT's advantages were achieved without compromising prescription dose delivery. These dosimetric advantages are particularly important in pediatric neuro-oncology, where tumors are often located adjacent to highly radiosensitive structures, and even small volumes of unintended high-dose exposure may result in long-term toxicity; consequently, a small improvement in dose distribution may meaningfully reduce the risk of late neurocognitive, endocrine, and sensory sequelae [1, 2, 9, 27].

The present dosimetric analysis of clinically delivered treatment plans is consistent with recent replanning dosimetric comparisons in the pediatric and adult brain radiotherapy literature. Zeng et al. [28] demonstrated superior conformity, homogeneity and normal tissue sparing using advanced VMAT techniques compared with IMRT in brain tumors, while Le Ba Thach et al. [29] reported similar gains when transitioning from 3D-CRT to VMAT in hippocampal avoidance whole brain radiotherapy. These retrospective replanning studies together

with our long-term institutional data, collectively reinforce the notion that VMAT offers a robust conformity advantage across diverse intracranial indications.

The radiation exposure to optic structures is associated with delayed-onset, often irreversible vision loss, with risk increasing as a function of both cumulative dose and proximity of the tumor target to the optic pathway, as demonstrated by Buket Kinaci-Tas et al. [30]. Although limited by sample size, the organ at risk (OAR) analysis revealed a consistent trend toward reduced maximum doses to critical structures with VMAT, particularly within the optic pathway and pituitary region. The observed reduction in optic chiasm maximum dose (5339 cGy → 4673 cGy) is of particular clinical importance, as the optic apparatus exhibits a steep dose–response relationship, and relatively modest dose reductions may translate into substantial improvements in long-term visual preservation [9, 27, 31].

Similarly, the tendency toward lower pituitary doses carries significant implications for endocrine outcomes. Growth hormone deficiency remains one of the most frequent late effects following pediatric brain irradiation, often occurring at doses well below traditional tolerance thresholds [3, 4]. In this context, even non-significant but consistent dose lowering trends may be biologically and clinically meaningful, especially when considered over a population with long life expectancy. In pediatric medulloblastoma treated with craniospinal irradiation and in adult FBRT cases, our findings are consistent with previous reports [32–34] showing that VMAT, compared with conventional three-dimensional conformal radiotherapy (3D-CRT), significantly improves dose conformity and homogeneity while reducing intermediate-to high-dose exposure to multiple organs at risk.

Our data suggest that VMAT delivers a pronounced reduction in high-dose spill outside the target volume, although it may broaden the spatial distribution of low-dose radiation. Given the stronger evidence linking high dose exposure to deterministic late toxicities such as neurocognitive decline, visual impairment, and endocrine dysfunction, the tradeoff may favor VMAT in pediatric FBRT [35]. This interpretation is consistent with recent reviews emphasizing that, in contemporary photon radiotherapy, the mitigation of high dose exposure to critical structures likely outweighs the theoretical risks associated with low dose spread, particularly when long term functional outcomes are prioritized [9].

The primary objective of this study was to evaluate dosimetric performance. In addition to the dosimetric comparison, an overall survival analysis was performed to assess whether the observed improvements in plan quality with VMAT were associated with differences in clinical outcomes. The limited availability of all follow-up data restricts the statistical power of the survival analysis. Based on this cohort data no statistically significant difference in overall survival was observed between the 3D-CRT and VMAT cohorts ($p = 0.26$). In general, the overall survival in pediatric brain tumors is influenced by numerous factors beyond radiotherapy technique, including tumor histology, molecular characteristics, disease stage, extent of surgical resection and systemic therapy [36–39]. In the present limited cohort, the effects of these prognostic factors were unlikely to have been fully averaged out between the treatment groups; therefore, the result of the survival analysis should be regarded as complementary to the dosimetric findings.

Another limitation of this study is the small number of cases available for maximum organ-at-risk (OAR) dose comparison due to strict prescription dose uniformity criteria, together with residual heterogeneity in tumor location and target geometry, which may have influenced OAR dose distributions independently of treatment technique. Furthermore, no toxicity, neurocognitive, endocrine, or visual outcome data were available to directly correlate the observed dosimetric differences with clinical outcomes. To address these limitations, the authors are planning a follow-up study to systematically investigate the relationship between dosimetric parameters and long-term clinical outcomes. Despite these limitations, the study has notable strengths that enhance the reliability of its conclusions.

This study expands the existing literature by providing a comprehensive 15-year institutional analysis of the transition from 3D-CRT to VMAT in pediatric focal brain radiotherapy, based on clinically delivered treatments rather than retrospective replanning. Confirming the superior dosimetric performance of VMAT—including improved conformity, homogeneity, reduced high-dose spillage, and lower doses to selected organs at risk. Therefore, the observed dosimetric advantages reflect not only the theoretical capabilities of VMAT but also its practical implementation under real-world clinical conditions. Given the long-life expectancy of these patients, thus these findings support the continued use of advanced conformal radiotherapy techniques and provide a basis for future studies on late toxicity, neurocognitive and endocrine outcomes.

Overall, our study demonstrates that the application of VMAT in pediatric focal brain irradiation is not merely a technological advancement, but a notable improvement in the precision of dose distribution. Our results support the clinical use of VMAT, with the potential to reduce late toxicity in this vulnerable patient population.

Data availability statement

The raw data supporting the conclusions of this article will be made available by the authors, without undue reservation.

Ethics statement

This study was conducted in accordance with the Declaration of Helsinki. The study protocol was reviewed and approved by the Medical Research Council Scientific and Research Ethics Committee (ETT-TUKEB, Hungary; approval number: BM/6038-1/2024, date of approval: 7 March 2024). Due to the retrospective nature of the study and the use of fully anonymized dosimetric data, the requirement for informed consent was waived by the Ethics Committees.

Author contributions

Conceptualization, MS, ÁK, and IS; methodology, MS, ÁK, and IS; software, GM; investigation, DK-S and GM; resources, ÁK and IS; data curation, DK-S and GM; writing – original draft preparation, DK-S and GM; writing – review and editing, MS, KG, JP, LM, CK, ÁK, and IS; visualization, DK-S and GM; supervision, ÁK and IS; funding acquisition, ÁK and CK. All

authors contributed to the article and approved the submitted version.

Funding

The author(s) declared that financial support was not received for this work and/or its publication.

Conflict of interest

The author(s) declared that this work was conducted in the absence of any commercial or financial relationships that could be construed as a potential conflict of interest.

Generative AI statement

The author(s) declared that generative AI was used in the creation of this manuscript. ChatGPT (OpenAI, GPT-5.5) and Microsoft Copilot were used for English grammar checking during manuscript preparation, and for Python and MATLAB code review for automated data extraction and statistical analysis. The authors are fully responsible for the content and analyses.

Any alternative text (alt text) provided alongside figures in this article has been generated by Frontiers with the support of artificial intelligence and reasonable efforts have been made to ensure accuracy, including review by the authors wherever possible. If you identify any issues, please contact us.

References

1. Söderström H, Walfridsson A, Martinsson U, Isacsson U, Brocki K, Kleberg JL, et al. Neurocognition and mean radiotherapy dose to vulnerable brain structures: new organs at risk? *Radiat Oncol* (2023) 18:132. doi: 10.1186/s13014-023-02324-2

2. Ajithkumar T, Price S, Horan G, Burke A, Jefferies S. Prevention of radiotherapy-induced neurocognitive dysfunction in survivors of paediatric brain tumours: the potential role of modern imaging and radiotherapy techniques. *Lancet Oncol* (2017) 18:e91–e100. doi: 10.1016/S1470-2045(17)30030-X

3. Vatner RE, Niemierko A, Misra M, Weyman EA, Goebel CP, Ebb DH, et al. Endocrine deficiency as a function of radiation dose to the hypothalamus and pituitary in pediatric and young adult patients with brain tumors. *J Clin Oncol* (2018) 36:2854–62. doi: 10.1200/JCO.2018.78.1492

4. Lövgren I, Abravan A, Bryce-Atkinson A, van Herk M. The late effects of cranial irradiation in childhood on the hypothalamic–pituitary axis: a radiotherapist's perspective. *Endocr Connect* (2022) 11:e220298. doi: 10.1530/EC-22-0298

5. Cohen-Cutler S, Wong K, Mena V, Sianto K, Wright MA, Olch A, et al. Hearing loss risk in pediatric patients treated with cranial irradiation and cisplatin-based chemotherapy. *Int J Radiat Oncology*Biology*Physics* (2021) 110:1488–95. doi: 10.1016/j.ijrobp.2021.02.050

6. Gehin W, Lassalle B, Salleron J, Anxionnat R, Peiffert D, Marchesi V, et al. Dosimetric predictive factors for facial nerve paralysis after cyberknife® stereotactic radiotherapy for vestibular schwannomas: a single institution experience of 88 patients. *Radiother Oncol* (2023) 181:109519. doi: 10.1016/j.radonc.2023.109519

7. Rao AD, Ladra M, Dunn E, Kumar R, Rao SS, Sehgal S, et al. A road map for important centers of growth in the pediatric skeleton to consider during radiation therapy and associated clinical correlates of radiation-induced growth toxicity. *Int J Radiat Oncology*Biology*Physics* (2019) 103:669–79. doi: 10.1016/j.ijrobp.2018.10.026

8. Rasmussen CM, Laack NN, Salinas TJ, Muller OM, Lee SKY, Carr AB. In skeletally immature children receiving radiation for craniofacial pathology, is success of subsequent orthopedic treatment of maxillary transverse skeletal deficiency affected by inclusion of the midpalatal suture in proton beam volume? *Adv Radiat Oncol* (2021) 6:100671. doi: 10.1016/j.adro.2021.100671

9. Milano MT, Marks LB, Olch AJ, Yorke ED, Jackson A, Bentzen SM, et al. Comparison of risks of late effects from radiation therapy in children *versus* adults: insights from the QUANTEC, HyTEC, and PENTEC efforts. *Int J Radiat Oncol Biol Phys* (2024) 119:387–400. doi: 10.1016/j.ijrobp.2023.08.066

10. Padovani L, André N, Constine LS, Muracciole X. Neurocognitive function after radiotherapy for paediatric brain tumours. *Nat Rev Neurol* (2012) 8:578–88. doi: 10.1038/nrneurol.2012.182

11. Moussawi N, Kanawati WE, El Balaa H. Plan quality metrics to assess the effectiveness of 3DCRT and VMAT treatment strategies for Left- sided breast cancer patients. *Health Technol (Berl)* (2025) 15:449–61. doi: 10.1007/s12553-025-00956-w

12. Fraass BA, McShan DL, Ten Haken RK. More than pretty pictures: 3-D treatment planning and conformal therapy. *Med Phys* (2023) 50:45–9. doi: 10.1002/mp.16117

13. Freihat O, Sipos D, Kotb R, Aamir M, Solymosi D, Gál K, et al. Three-dimensional conformal therapy vs. intensity modulated radiation therapy in GBM: survival, dosimetry, and side effects a systematic review and meta-analysis. *Front Phys* (2025) 13:1632620. doi: 10.3389/fphy.2025.1632620

14. Otto K. Volumetric modulated arc therapy: IMRT in a single gantry arc. *Med Phys* (2008) 35:310–7. doi: 10.1118/1.2818738

15. Teoh M, Clark CH, Wood K, Whitaker S, Nisbet A. Volumetric modulated arc therapy: a review of current literature and clinical use in practice. *Br J Radiol* (2011) 84:967–96. doi: 10.1259/bjr/22373346

16. Hall EJ, Wuu C-S. Radiation-induced second cancers: the impact of 3D-CRT and IMRT. *Int J Radiat Oncology*Biology*Physics* (2003) 56:83–8. doi: 10.1016/S0360-3016(03)00073-7

17. Moteabbed M, Yock TI, Paganetti H. The risk of radiation-induced second cancers in the high to medium dose region: a comparison between passive and scanned proton therapy, IMRT and VMAT for pediatric patients with brain tumors. *Phys Med Biol* (2014) 59:2883–99. doi: 10.1088/0031-9155/59/12/2883

18. Scaringi C, Agolli L, Minniti G. Technical advances in radiation therapy for brain tumors. *Anticancer Res* (2018) 38:6041–5. doi: 10.21873/anticanres.12954

19. Gong Y, Wang J, Bai S, Jiang X, Xu F. Conventionally-fractionated image-guided intensity modulated radiotherapy (IG-IMRT): a safe and effective treatment for cancer spinal metastasis. *Radiat Oncol* (2008) 3:11. doi: 10.1186/1748-717X-3-11

20. Prescribing R, Icru J Reporting photon-beam intensity-modulated radiation therapy (IMRT), 10 (2010). NP.3–NP. doi: 10.1093/jicru/ndq002

21. Shaw E, Kline R, Gillin M, Souhami L, Hirschfeld A, Dinapoli R, et al. Radiation therapy oncology group: radiosurgery quality assurance guidelines. *Int J Radiat Oncology*Biology*Physics* (1993) 27:1231–9. doi: 10.1016/0360-3016(93)90548-A

22. Paddick I. A simple scoring ratio to index the conformity of radiosurgical treatment plans. *J Neurosurg* (2000) 93(Suppl. 3):219–22. doi: 10.3171/jns.2000.93.supplement_3.0219

23. Mekki L, Acharya S, Ladra M, Lee J. Deep learning segmentation of organs-at-risk with integration into clinical workflow for pediatric brain radiotherapy. *J Appl Clin Med Phys* (2024) 25:e14310. doi: 10.1002/acm2.14310

24. Erdur AC, Rusche D, Scholz D, Kiechle J, Fischer S, Llorián-Salvador Ó, et al. Deep learning for autosegmentation for radiotherapy treatment planning: state-Of-the-art and novel perspectives. *Strahlentherapie und Onkologie* (2025) 201:236–54. doi: 10.1007/s00066-024-02262-2

25. Han EY, Kim G-Y, Rebueno N, Yeboa DN, Briere TM. End-to-End testing of automatic plan optimization using RayStation scripting for hypofractionated multimetastatic brain stereotactic radiosurgery. *Med Dosimetry* (2019) 44:e44–e50. doi: 10.1016/j.meddos.2018.12.006

26. Szalkowski G, Xu X, Das S, Yap P-T, Lian J. Automatic treatment planning for radiation therapy: a cross-modality and protocol study. *Adv Radiat Oncol* (2024) 9:101649. doi: 10.1016/j.adro.2024.101649

27. Constine LS, Marks LB, Milano MT, Ronckers CM, Jackson A, Hudson MM, et al. A user's guide and summary of pediatric normal tissue effects in the clinic (PENTEC): radiation dose-volume response for adverse effects after childhood cancer therapy and future directions. *Int J Radiat Oncol Biol Phys* (2024) 119:321–37. doi: 10.1016/j.ijrobp.2023.09.005

28. Zeng H, Zhong M, Chen Z, Tang S, Wen Z. A dosimetric comparison of non-coplanar volumetric modulated arc therapy and non-coplanar fixed field intensity modulated radiation therapy in hippocampus-avoidance whole-brain radiation therapy with a simultaneous integrated boost for brain metastases. *Front Oncol* (2025) 14:1428329. doi: 10.3389/fonc.2024.1428329

29. Thach LB, Thao MT, Nghia NV, My TN, Tai DT, Tamam N, et al. Hippocampal-avoidance whole-brain radiotherapy: dosimetric comparison of 3D-CRT, IMRT, and

VMAT for brain metastases from lung cancer. *Cancers (Basel)* (2025) 17:3744. doi: 10.3390/cancers17233744

30. Kinaci-Tas B, Alderliesten T, Verbraak FD, Rasch CRN. Radiation-induced retinopathy and optic neuropathy after radiation therapy for brain, head, and neck tumors: a systematic review. *Cancers (Basel)* (2023) 15:1999. doi: 10.3390/cancers15071999

31. Marks LB, Yorke ED, Jackson A, Ten Haken RK, Constine LS, Eisbruch A, et al. Use of normal tissue complication probability models in the clinic. *Int J Radiat Oncology*Biology*Physics* (2010) 76:S10–S19. doi: 10.1016/j.ijrobp.2009.07.1754

32. Gupta M, Kant R, Nautiyal V, Bisht J, Raghuvanshi S, Saini M, et al. Dosimetric comparison between three-dimensional conformal radiation therapy and intensity-modulated radiation therapy in the treatment of posterior fossa boost in medulloblastoma. *J Cancer Res Ther* (2017) 13:1027–31. doi: 10.4103/0973-1482.220416

33. Pollul G, Bostel T, Grossmann S, Akbaba S, Karle H, Stockinger M, et al. Pediatric craniospinal irradiation with a short partial-arc VMAT technique for medulloblastoma tumors in dosimetric comparison. *Radiat Oncol* (2020) 15:256. doi: 10.1186/s13014-020-01690-5

34. Zamani H, Saeb M, Monadi S, Alizade-Harakiyan M, Akhavan A, Khodaei A, et al. Dosimetric and radiobiological parameters in brain cancers: a comparison of IMRT and VMAT techniques. *Phys Open* (2026) 26:100362. doi: 10.1016/j.physo.2025.100362

35. Gade VKV. Early and late effects of radiotherapy in children. In: *Evidence Based Practice in Pediatric Radiation Oncology*. Singapore: Springer Nature Singapore (2025). p. 23–35.

36. Pollack IF, Agnihotri S, Broniscer A. Childhood brain tumors: current management, biological insights, and future directions. *J Neurosurg Pediatr* (2019) 23:261–73. doi: 10.3171/2018.10.PEDS18377

37. Lutz K, Jünger ST, Messing-Jünger M. Essential management of pediatric brain tumors. *Children* (2022) 9:498. doi: 10.3390/children9040498

38. Hatoum R, Chen J-S, Lavergne P, Shlobin NA, Wang A, Elkaim LM, et al. Extent of tumor resection and survival in pediatric patients with high-grade gliomas. *JAMA Netw Open* (2022) 5:e2226551. doi: 10.1001/jamanetworkopen.2022.26551

39. Viaene AN. Pediatric brain tumors: a neuropathologist's approach to the integrated diagnosis. *Front Pediatr* (2023) 11:1143363. doi: 10.3389/fped.2023.1143363